Journal of Neonatal Surgery
ISSN(Online): 2226-0439
Vol. 14, Issue 32s (2025)
https://www.jneonatalsurg.com

OPEN ACCESS

Conventional, Diffusion Weighted and Dynamic Contrast MRI in Evaluation of Oral Cavity and Pharyngeal Masses

Reham Samy Ahmed Sheta[*1], Rasha Mahmoud Dawoud[1], Al-Siagy Ali Salama[1], Alaa Mohamed Maria[2], Khaled Ismail Elshafey[1]

[1]Radiodiagnosis Department, Faculty of Medicine, Tanta University, Tanta, Egypt

[2]Clinical Oncology Department, Faculty of Medicine, Tanta University, Tanta, Egypt

[*]**Corresponding author:**

Reham Samy Ahmed Sheta

Cite this paper as: Reham Samy Ahmed Sheta, Rasha Mahmoud Dawoud, Al-Siagy Ali Salama, Alaa Mohamed Maria, Khaled Ismail Elshafey, (2025) Conventional, Diffusion Weighted and Dynamic Contrast MRI in Evaluation of Oral Cavity and Pharyngeal Masses. *Journal of Neonatal Surgery*, 14 (32s), 4491-4503.

ABSTRACT

Background: The oral cavity is a complicated anatomical region that can be impacted by various disease masses. Proper diagnosis and grading of the mass is crucial for treatment plan and prognosis. The use of added sequences as diffusion weighted MRI (DWI) and dynamic contrast enhanced MRI (DCE) is supposed to offer more accuracy in differentiation and staging of the masses. The aim of the present work was to estimate the diagnostic value of multi-parametric MRI in evaluation of oral or pharyngeal masses.

Methods: The prospective trial was carried out on 80 cases, aged from 18 to 62 years, both sexes, with suspected oral or pharyngeal mass. All patients were subjected to radiological and imaging evaluation including conventional MRI, DWI and DCE.

Results: 26 cases were malignant in nature, two of them were lymphoma. 26 cases were benign including inflammatory masses. Recurrent lesions were found in 16 cases. Post-operative fibrosis in the tumor bed with negative malignancy in pathology was found in 12 cases. Overall accuracy for diagnosis of masses was higher using multi parametric MRI than conventional MRI with 95% and 85.15% respectively. For differentiation of recurrent or residual masses from post-operative fibrosis, Overall accuracy was 86.67% and 66.67% in multi parametric MRI and conventional MRI respectively. T and N staging systems were used for malignant masses. Accuracy of staging of the truly diagnosed cases was 80% using conventional MRI, and 91.6% using multiparametric MRI. For N staging, accuracy of conventional MRI was 80.3%. While accuracy of multipara metric MRI was 91.6%.

Conclusions: Multi parametric MRI use can enhance the diagnostic accuracy of conventional MRI regarding nature of the masses, staging of malignant ones and discrimination of recurrent/ residual masses from post therapeutic changes.

Keywords: *Diffusion Weighted Imaging, Dynamic Contrast Enhancement, Magnetic Resonance Imaging, Multi Parametric, Oral or Pharyngeal Masses*

1. INTRODUCTION

The oral cavity and pharynx constitute a complicated anatomical region, allocated into numerous spaces and subspaces. This region can be susceptible by various developmental, inflammatory, and neoplastic diseases (1).

The preoperative differential diagnosis of oral or pharyngeal lesions is critical as the treatment approach differs depending on the pathology: squamous cell carcinoma and some other malignant tumors are typically managed with surgical resection followed by radiotherapy, whereas lymphoma is primarily treated with chemotherapy. Benign tumors are usually surgically resected, with a generally favorable prognosis. Therefore, accurately differentiating between benign and malignant lesions, and among different subgroups of lesions is essential for proper treatment planning. However, the complex anatomical nature of this region and the movement of structures during imaging present challenges in achieving a precise diagnosis. (2)

Among the available imaging techniques, Magnetic Resonance Imaging (MRI) is chosen because of its greater soft tissue contrast resolution, which aids in distinguishing tumor margins from surrounding tissues. MRI examines morphology, signal intensity, and enhancing patterns of lesions. (3)

The dilemma of the accuracy of conventional MRI in differentiation of benign from malignant lesions as well as, tumor recurrence from post treatment changes is still unsolved. The post-surgical disruption of normal anatomy, plus the edema and fibrosis caused by radio and chemotherapy, impede appropriate interpretation of standard MRI imaging, making discrimination between local recurrence and post-treatment changes problematic. This has necessitated further research into the diagnostic value of additional MRI sequences, such as diffusion-weighted MRI and dynamic contrast-enhanced (DCE) MRI. (4)

The aim of the present work was to estimate the diagnostic value of multiparametric MRI in assessing oral and pharyngeal masses.

Sample size

The sample size was estimated based on a moderate agreement (k = 0.537) for the T stage among clinical and MRI staging, as opposed to a poor agreement (k = 0.085) between clinical and histopathological staging, as showed in a prior research (Singh et al., 2017) (5). Considering a 0.05 α error and an 80% study power, ten additional cases were included to account for potential dropouts. Consequently, a total of 60 cases or more were allocated.

2. PATIENTS AND METHODS

The current prospective trial was carried out on 80 cases with oral or pharyngeal masses who were referred to the Radiodiagnosis and Medical Imaging Department at Tanta University Hospital. The study spanned a two-year period, from August 2022 to July 2024.

Cases were excluded if they have contraindication to MRI examination or intravenous contrast media injection, including impaired renal function with a GFR lower than 35 mL/min/1.73 m², a history of allergy to contrast media, or refusal to undergo the examination.

After a complete medical history was obtained, all patients underwent a clinical assessment that included vital signs evaluation, assessment of consciousness level, local examination of the oral cavity, and renal function tests.

All MRI examinations were performed using a GE Signa Explorer 1.5T scanner with a head and neck coil at the Radiodiagnosis Department of Tanta University Hospital. Each patient underwent conventional pre-contrast MRI, diffusion-weighted imaging (DWI), and post-contrast dynamic studies. The total average scan time was approximately 40 minutes, with no sedation or anesthesia administered.

Protocol of MRI imaging:

All cases were examined using a standardized MRI protocol that included multiple sequences. Conventional MRI sequences began with scout three-plane T1-weighted images for localization. Axial T2-weighted spin-echo sequences with high-resolution thin cuts were acquired for the oral cavity and/or pharynx, using parameters of TR/TE 2000/200 ms, a flip angle of 90°, a field of view (FOV) of 180 mm, a matrix size of 256 × 256, a slice thickness of 4 mm, and an inter-slice gap of 1.8 mm. Additional axial T2 fat-saturated sequences were obtained with TR/TE 4412/20 ms, a flip angle of 90°, an FOV of 180 mm, a matrix size of 256 × 256, a slice thickness of 5 mm, and an inter-slice gap of 0.5 mm. Axial T1-weighted images were acquired using TR/TE 600/30 ms, an FOV of 250 mm, a matrix size of 256 × 256, a slice thickness of 4 mm, and an inter-slice gap of 0.5 mm. Coronal T1-weighted spin-echo sequences were performed with TR/TE 528.4/15 ms, a flip angle of 69°, an FOV of 250 mm, a matrix size of 256 × 256, a slice thickness of 4 mm, and an inter-slice gap of 0.5 mm. Coronal short tau inversion recovery (STIR) sequences were also included with TR/TE 4412/20 ms, a flip angle of 90°, an FOV of 250 mm, a matrix size of 256 × 256, a slice thickness of 4 mm, and an inter-slice gap of 0.5 mm.

Magnetic resonance diffusion imaging was performed utilizing a multi-section single-shot echo-planar imaging (EPI) sequence with TR/TE/NEX parameters of 7473/79 ms/1, a field of view of 230 mm, a matrix size of 128 × 128, a section thickness of 3 mm, and a section gap of 0 mm. Diffusion weighted imaging was conducted with b-values of 500 and 1000 s/mm², and the signal intensity of the lesion was evaluated at b = 1000. The apparent diffusion coefficient (ADC) maps were automatically estimated by the MRI software. Regions of interest (ROIs) were manually placed along the margins of the lesions on the ADC maps, using the corresponding diffusion-weighted images as references. The ADC values were then averaged and expressed in units of 10^{-3} mm²/s.

Post-contrast MRI sequences were obtained using a dynamic study performed following bolus injection of 0.1 mmol/kg body weight of gadolinium-DTPA. The dynamic imaging was done by utilizing a 2D T1-weighted gradient-echo sequence, consisting of one pre-contrast series followed by seven successive post-contrast series capturing the early arterial, late arterial, venous, and delayed phases at 15-second intervals, with a total acquisition time of 240 seconds. The acquisition factors included TR 4.8 ms, TE 2.3 ms, a flip angle of 10°, a matrix size of 172 × 163, a field of view of 190 mm, and a slice thickness of 3 mm.

MRI images analysis:

Conventional MRI, DWI, and post-contrast dynamic MRI images were analyzed separately in different sessions and in

random order using the GE Extended Workstation.

Interpretation of DWI-MRI images:

Both qualitative and quantitative evaluations, including ADC value analysis, were performed. Lesions displaying a high signal on DWI were considered to have free diffusion and a low signal on the ADC map were considered to have restricted diffusion

Interpretation of DCE-MRI images:

- Data analysis was conducted on a workstation, where multiple regions of interest (ROIs) were drawn on the mass lesions, avoiding cystic or necrotic parts of the enhancing lesions as much as possible to generate a color-coded map. The time-signal intensity (TSI) curve was generated then reviewed qualitatively. Three types of curves were identified (figure1): Type I revealed a slow rise with no definite peak, Type II exhibited moderate initial improvement followed by stable enhancement, and Type III demonstrated rapid steep early enhancement with early rapid washout. (6)

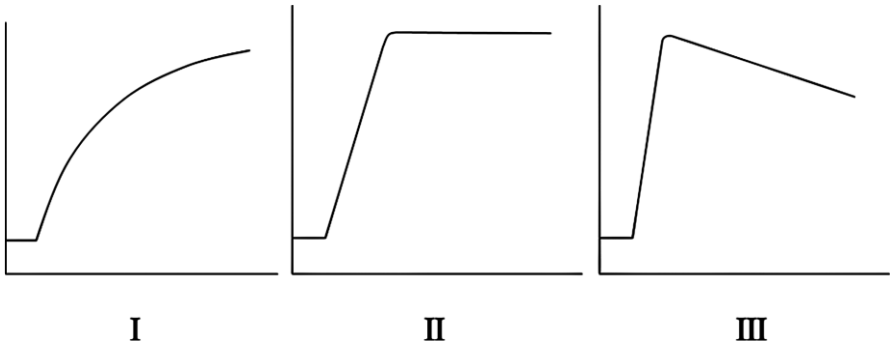

Figure 1: Types of time-signal intensity curve: type I, progressive gradual enhancement; type II, stable plateau enhancement; and type III, rapid rise and relative rapid washout curve

Standard of reference:

Laboratory findings and histological investigation were used to determine if lesions were true or false, positive or negative.

Statistical analysis:

The data were processed and analyzed with the IBM SPSS software program version 20.0 (Armonk, NY: IBM Corp). Numbers and percentages were employed to describe qualitative data, and the Shapiro-Wilk test was utilized to ensure that the distribution was normal. Quantitative data were described using the terms range (minimum and maximum), mean, standard deviation, median, and interquartile range (IQR). The significance of the acquired results was determined at a 5% level.

3. RESULTS

The study involved 80 cases with mean age of 45.18 years extended from 18 to 62 years. The majority were males (57.5%). Left-sided lesions were the most common, take place in 38 cases (47.5%), followed by right-sided lesions in 26 patients (32.5%), while midline lesions were the least frequent, seen in 16 cases (20%). Patient's demographic data, clinical symptoms, site of lesion and pathology were scheduled in **table 1.**

Table 1: Distribution of the studied cases according to demographic data, clinical symptoms, site of lesion and pathology

		N=80
Age (years)		45.18 ± 12.20
Sex	**Male**	46(57.5%)
	Female	34(42.5%)
Clinical symptoms	**Sensation of swelling/mass**	50(62.4%)
	Local Pain	26(32.5%)

	Otalgia	8(10.0%)
	Difficulty in swallowing	22(27.5%)
	Nasal congestion	12(15.0%)
	Fever	8(10.0%)
Site of lesion	**Floor of mouth**	6(7.5%)
	Nasopharynx	14(17.5%)
	Gingiva	6(7.5%)
	Submandibular and submental region	4(5.0%)
	Tongue	34(42.5%)
	Upper lip	4(5.0%)
	Lower Lip	4(5.0%)
	Angle of mouth	2(2.5%)
	Hypopharynx	2(2.5%)
	Hard palate	2(2.5%)
	Oropharynx	2(2.5%)
Pathology	**Chronic infection**	4(5.0%)
	TB granuloma	2(2.5%)
	Ranula	4(5.0%)
	Dermoid cyst	2(2.5%)
	Haemagioama	2(2.5%)
	Thornwaldet cyst	2(2.5%)
	Fibroma	2(2.5%)
	Pleomorphic adenoma	8(10.0%)
	Adenoid cystic carcinoma	2(2.5%)
	Lymphoma	2(2.5%)
	Mucoepidermoid carcinoma	4(5.0%)
	SCC	14(17.5%)
	Nasopharyngeal keratinizing adenocarcinoma	4(5.0%)
	Recurrent SCC	16(20.0%)
	Post-operative fibrosis	12(15.0%)

Masses were categorized regarding its pathology into inflammatory, benign, malignant and post-operative changes. Radiological characterization of different type of masses was enumerated in **table 2.**

Table 2: Radiological characterization of different type of masses

		Inflammatory (n=6)	Benign (n=20)		Malignant (n=24)	Lymphoma (n=2)	Recurrent /residual malignancy (n=16)	Post treatment granulation tissue /fibrosis (n=12)
Borders	**Well defined**	--	16(80%)		4(16.7%)	--	--	--
	Fairly defined	2(33.3%)	4(20%)		--	--	6(37.5%)	8(66.7%)
	Ill defined	4(66.7%)	--		20(83.3%)	2(100%)	10(62.5%)	4(33.3%)
infiltration	**Yes**	6(100%)	--		20(83.3%)	2(100%)	12(75%)	4(33.3%)
	No	--	20(100%)		4(16.7%)	--	4(25%)	8(66.7%)
T1WI	**High signal**	--	4(20%)		--	--	--	--
	Intermediate	--	4(20%)		10(58.3%)	--	6(37.5%)	8(66.7%)
	Low	6(100%)	12(60%)		14(58.3%)	2(100%)	10(62.5%)	4(33.3%)
T2WI	**High signal**	2(33.3%)	16(80%)		20(83.3%)	2(100%)	12(75%)	8(66.7%)
	Intermediate	--	4(20%)		4(16.7%)	--	4(25%)	4(33.3%)
	Low	4(66.7%)	--		--	--	--	--
T2 Fat sat WI	**High signal**	--	16(80%)		20(83.3%)	2(100%)	14(87.5%)	10(83.3%)
	Intermediate	6(100%)	4(20%)		4(16.7%)	--	2(12.5%)	2(16.7%)
Diffusion weighted MRI	**Free**	5(83.3%)	8(100%)	12(100%)	2(8.3%)	--	2(12.5%)	10(83.3%)
	Restricted	1(16.7%)	--	--	22(91.7%)	2(100%)	14(87.5%)	0(16.7%)
	Mean ADC value	0.98	2.3	1.48	0.97	0.7	1.1	1.53
TIC	**Type I**	5(83.3%)	20(100%)		--	--	--	8(66.7%)
	Type II	1(16.7%)	--		4(16.6%)	--	4(25%)	4(33.3%)
	Type III	--	--		20(83%)	2(100%)	12(75%)	--

Data is presented as mean or frequency (%). MRI: Magnetic resonance imaging. TIC: Time intensity curve.

Conventional MRI Interpretation

Conventional MRI accurately diagnosed 68 out of 80 cases when referenced against histopathology. Four cases were misdiagnosed as benign instead of malignant based on MRI characteristics, as they appeared small with well-defined outlines

and no obvious infiltration of surrounding structures. These lesions displayed a low to intermediates signal on T1WI and an intermediate to high signal on T2WI/T2FATSAT. Among post-treatment cases, four lesions were falsely interpreted as recurrent masses rather than post-treatment granulation tissue or fibrosis based on MRI characteristics, showing ill-defined outlines with radiological infiltration of surrounding structures and displaying a low to intermediate signal on T1WI with an intermediate to high signal on T2WI/FATSAT. Conversely, another four cases were incorrectly interpreted as post-treatment granulation tissue or fibrosis rather than recurrent masses, despite showing fairly defined masses without significant radiological infiltration of surrounding structures and displaying similar signal characteristics. **(Table 3)**

Multiparametric MRI Interpretation

Multiparametric MRI demonstrated higher diagnostic accuracy, correctly diagnosing 76 out of 80 cases when referenced against histopathology. Among the four misclassified cases in the post-treatment group, two were mistakenly identified as recurrent masses instead of post-treatment granulation tissue or fibrosis based on MRI characteristics. However, pathological evaluation confirmed post-treatment changes, with MRI showing an ill-defined mass with clear radiological infiltration of surrounding structures, a low to intermediate signal on T1WI, an intermediate to high signal on T2WI/T2FATSAT, restricted diffusion, and a Type B curve. The remaining two cases were misclassified as post-treatment granulation tissue or fibrosis instead of recurrent masses, despite exhibiting fairly defined outlines, no significant radiological infiltration, a low to intermediate signal on T1WI, an intermediate to high signal on T2WI/T2FATSAT, free diffusion, and a Type B curve. **(Table 3)**

After exclusion of infection masses, ADC values data from diffusion weighted imaging was used to draw ROC curve (figure 2). A cut-off value was determined to be utilized to differentiate among benign and malignant masses. It was found to be 1.2 x 10 ^{x3}. Below this measurement was considered malignant and above was considered benign.

Overall accuracy were higher when use multi parametric MRI than conventional MRI. Overall accuracy was 95% and 85.15% in multi parametric MRI and conventional MRI respectively. Sensitivity, specificity, positive prediction value and negative prediction value were varied according MRI different modalities as described in table 4

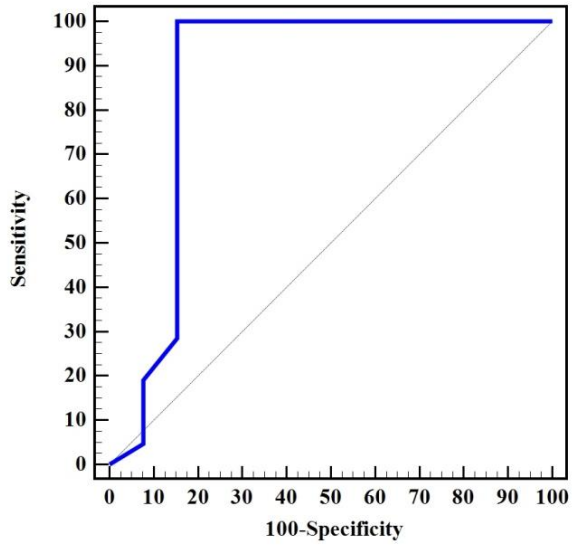

Figure 2: ROC curve for ADC to discriminate Malignant from Benign cases

Table 3: Accuracy of conventional MRI and multi-parametric MRI over the study in reference to pathology

Conventional MRI		
	Accurate diagnosis (n=68)	**False diagnosis (n=12)**
Inflammatory mass (n=3)	6(100.0%)	--
Benign masses (n=10)	20(100.0%)	--
Malignant masses (n=12)	20(83.3%)	4(16.7%)

Lymphoma (n=1)	2(100.0%)	--
Recurrent /residual malignancy (n=8)	12(75.0%)	4(25.0%)
Post treatment granulation tissue /fibrosis (n=6)	8(66.7%)	4(33.3%)
Multi-parametric MRI		
	Accurate diagnosis (n=76)	**False diagnosis (n=4)**
Inflammatory mass (n=3)	6(100.0%)	--
Benign masses (n=10)	20(100.0%)	--
Malignant masses (n=12)	24(100.0%)	--
Lymphoma (n=1)	2(100.0%)	--
Recurrent /residual malignancy (n=8)	14(87.5%)	2 (12.5%)
Post treatment granulation tissue /fibrosis (n=6)	10(83.3%)	2 (16.7%)

Data is presented as frequency (%). MRI: magnetic resonance imaging.

Table 4: Agreement (sensitivity, specificity and accuracy) for different MRI techniques

	Conventional MRI (n=80)	**Multi parametric MRI (n=80)**
True Positive	34	40
False Positive	4	2
True Negative	34	36
False Negative	8	2
Sensitivity (%)	80.9	95.2
Specificity (%)	89.4	94.7
PPV (%)	89.4	94.7
NPV (%)	80.9	95.2
Overall Accuracy (%)	85.15	95

In our study on 80 patients, 24 cases were diagnosed as primary malignant lesions based on histopathology of different pathological lesions. These cases were staged for local tumor extension (T) and regional nodal spread (N). For T staging, 20 patients were accurately diagnosed as malignant cases using conventional MRI, all 24 patients were correctly identified as malignant cases using multipara metric MRI. Accuracy of staging of the truly diagnosed cases was 16 over 20 case (80%) using conventional MRI, and 22 over 24 case (91.6%) using multiparametric MRI . For N staging, accuracy of conventional MRI was 80.3%. While, accuracy of multipara metric MRI was 91.6%. Tables 5, 6 and 7.

Table 5: pathological T and N staging of malignant masses:

Pathological T staging (n=24)	**T1**	6(25.0%)
	T2	6(25.0%)
	T3	4(16.7%)

	T4	8(33.3%)
Pathological N staging (n=24)	**N0**	10(41.7%)
	N1	4(16.7%)
	N2a	2(8.3%)
	N2b	2(8.3%)
	N3a	4(16.7%)
	N3b	2(8.3%)

Table 6: Accuracy of the studied cases according to radiological T staging in reference to histopathology

		Accurate staging (n=16)	**Up-staging (n=2)**	**Down-staging (n=2)**
Conventional MRI (n=20)	**T1**	2(12.5%)	0(0.0%)	0(0.0%)
	T2	4(25.0%)	0(0.0%)	2(100.0%)
	T3	2(12.5%)	2(100.0%)	0(0.0%)
	T4	8(50.0%)	0(0.0%)	0(0.0%)
		Accurate staging (n=22)	**Up-staging (n=0)**	**Down-staging (n=2)**
Multi parametric MRI (n=24)	**T1**	6(27.3%)	0(0.0%)	0(0.0%)
	T2	4(18.2%)	0(0.0%)	2(100.0%)
	T3	4(18.2%)	0(0.0%)	0(0.0%)
	T4	8(36.3%)	0(0.0%)	0(0.0%)

Data is presented as frequency (%).

Table (7): Distribution of the studied cases according to radiological N staging:

	N staging				Sensitivity	Specificity	PPV	**NPV**	**Accuracy**
	Negative (n = 6)		**Positive (n = 14)**						
	No.	**%**	**No.**	**%**					
Conventional MRI									
Negative	4	66.7	2	14.3	85.7	66.7	85.7	66.7	80.3
Positive	2	33.3	12	85.7					
Multi parametric MRI									
Negative	10	100	2	14.2	100	83.3	85.7	100	91.6
Positive	0	0	12	85.7					

PPV: Positive predictive value

Post-Treatment Cases and NIRADS Classification

Among 28 suspicious post-treatment cases, the NIRADS system was applied, classifying 14 cases (50%) as NIRADS 3, 4 cases (14.3%) as NIRADS 2, and 10 cases (35.7%) as NIRADS 1. Statistical analysis for recurrent masses showed that multiparametric provided greater overall accuracy (85.4%) compared to conventional MRI (70.8%). **(table 8)**

Table 8: Agreement for different MRI techniques in post treatment masses

	Conventional MRI (n=28)	Multi parametric MRI (n=28)
True Positive	12	14
False Positive	4	2
True Negative	8	10
False Negative	4	2
Sensitivity (%)	75	87.5
Specificity (%)	66.67	83.33
PPV (%)	75	87.5
NPV (%)	66.67	83.33
Overall Accuracy (%)	70.8	85.4

Case 1: A 45 –years – old female patient presented by right sided tongue mass. **Diagnosis:** Right sided hemi-tongue ill-defined soft tissue mass lesion, crossing midline with depth of invasion 2.5cm with ipsi-lateral suspicious lymph node. Neoplastic mass with stage T4N1. **Diagnosis:** Right hemi tongue neoplastic mass lesion with metastatic ipsi-lateral level II lymph node with diffusion restriction and post contrast type III washout curve. Multi- parametric MRI staging = T4N1. **Pathology:** Proved pathologically was poor in differentiating squamous cell carcinoma stage T4N1. **Figure 3**

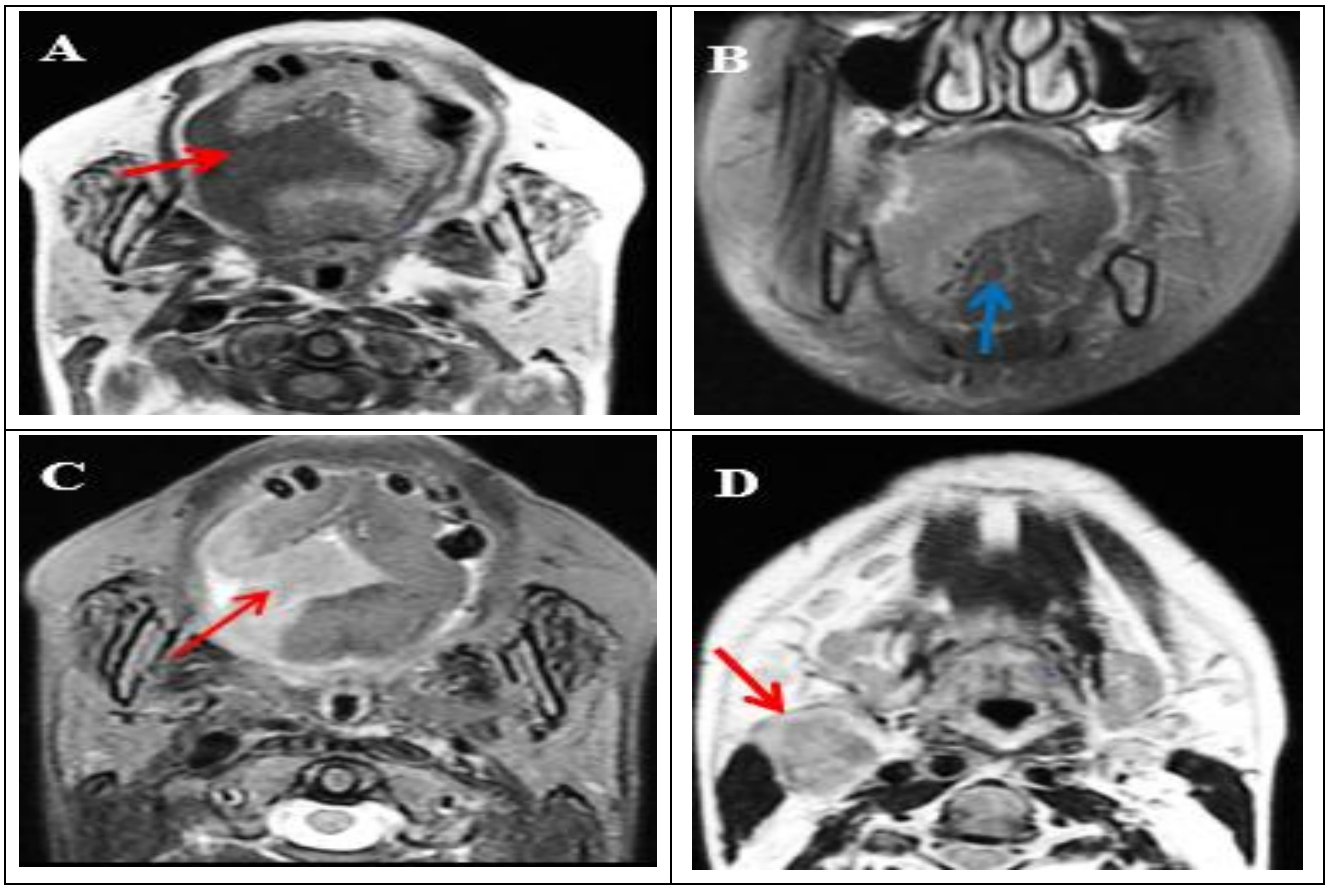

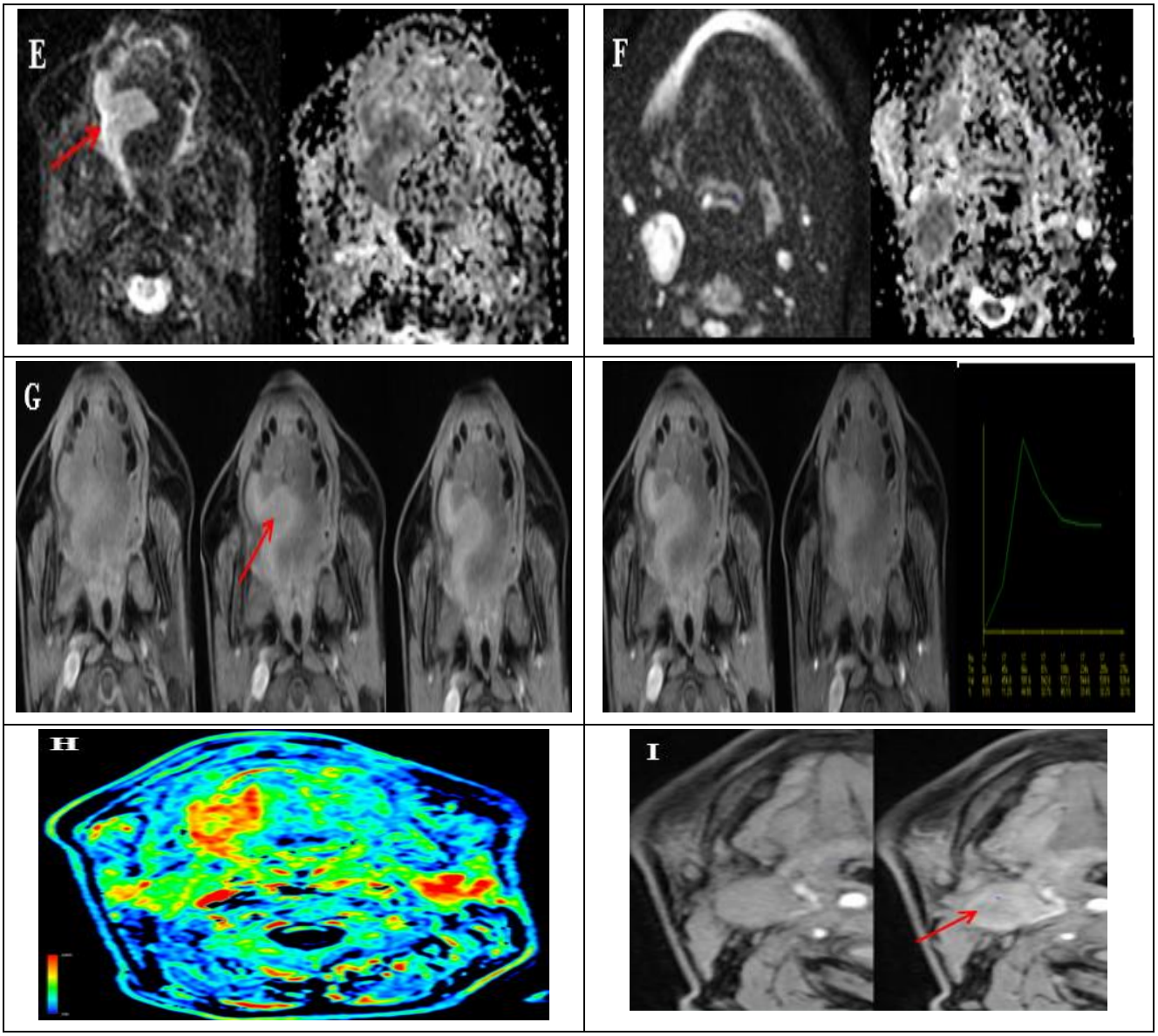

Figure 3: (A) Axial T1WI, (B) coronal T2FATSAT, (C) Axial T2WI FAT SAT: Ill-defined right hemi-tongue mass lesion (red arrow) with altered signal intensity display low T1WI, high T2W/PD seen extending to left side crossing midline by about 9mm also extending to right genoglossus muscle (blue arrow) . Depth of invasion: 2.5 cm, (D) Axial T2WI at level of lymph node: large ipsilateral level II enlarged irregular heterogeneous lymph node, (H) Color map showing red color of lesion denoting strong enhancement, (I) Ipsilateral enlarged lymph nodes. Ipsilateral level Ib lymph node that showed post contrast in homogenous enhancement with non-enhancing center.

4. DISCUSSION

The oral cavity and pharyngeal regions pose significant challenges for radiological diagnosis due to their complex anatomy, including soft tissues, glandular structures, and adjacent osseous components. (7)

The global occurrence of head and neck cancer is nearly 14 per 100,000, accounting for 16% to 40% of malignancies worldwide. A proper diagnosis is essential for treatment planning, prognosis estimation, treatment outcome evaluation, inter-center communication, and ongoing research in oncology. (8)

In the present study, the rule of multi parametric MRI use was evaluated in diagnosis of oral or pharyngeal masses.

Regarding diagnosis accuracy:

Conventional MRI is useful for diagnosing head and neck tumors although it has limitations in distinguishing benign from malignant lesions. Physiological lesion properties can be assessed using kinetic studies post-contrast injection. In this study,

multiparametric MRI demonstrated higher overall accuracy (95%) compared to conventional MRI (85.15%). This aligns with Moreira et al. (9), who conducted a meta-analysis on MRI accuracy for oral cancer diagnosis. They found that diffusion-weighted MRI (DW-MRI) had 76.4% global sensitivity and 91.3% specificity, while dynamic contrast-enhanced MRI (DCE-MRI) had 84.0% global sensitivity and 89.5% specificity of. Conventional MRI had 72.5% global sensitivity and 86.6% specificity.

Several studies have explored the combination of MRI modalities to improve diagnostic accuracy. Zhang et al. (10) examined the diagnostic role of diffusion-weighted MRI (DW-MRI) in hypopharyngeal carcinoma and found that the sensitivity, specificity, and accuracy of conventional MRI were 97.5%, 66.7%, and 89.1%, respectively. In contrast, the sensitivity and specificity of added DW-MRI were 100% and 75%, respectively. Dong et al. (11) investigated the added value of dynamic contrast-enhanced (DCE) MRI in differentiating squamous cell carcinoma of the head and neck and reported a diagnostic accuracy of 92.9%, sensitivity of 95.0%, and specificity of 90.9%.

Regarding malignant masses t staging :

Regarding malignant mass T-staging, our study employed T-staging to assess the depth of invasion (DOI) in malignant lesions. Using conventional MRI, the overall accuracy was 80%, with two patients being falsely downstaged and another two falsely upstaged. In contrast, multi-parametric MRI yielded an overall accuracy of 91.7%, with only two patients being falsely downstaged. This aligns with findings by **Singh et al.,** (5) that showed a good/substantial agreement for the T staging (tumor depth and width) between MRI and pathological measurements. With accurate final staging in 19 out of 22 patients who underwent surgery (accuracy 86.36 %)

Park et al. (12) assessed 114 cases with oral and oropharyngeal squamous cell carcinoma (SCC), including 49 cases of oral tongue SCC, and found a strong correlation between MRI and histologic DOI, with an accuracy of 94.9%. Similarly, Alsaffar et al. (13) demonstrated a robust correlation among MRI and histologic DOI in 49 patients of oral tongue cancer, yielding an accurate categorical staging in 46 out of 49 cases, with an overall accuracy of 93.87%. Guo et al. (14) reported that quantitative DCE-MRI for staging of tongue SCC achieved 64.3% sensitivity, 82.6% specificity, 81.8% positive predictive value (PPV), 65.5% negative predictive value (NPV), and 72.5% overall accuracy.

Other studies have used combinations of MRI modalities to enhance staging accuracy. Tang et al. (15) showed that the staging accuracy of tongue SCC using multi-parametric MRI was 86.9%. Differences in MRI sequences may explain some discrepancies in staging, particularly regarding overestimation of tumor size. False overestimation is largely related to tumor shrinkage postresection, which affects oral cavity subsites. Goel V. et al. (16) noted discrepancies between histologic and radiologic thicknesses because of shrinkage of specimen during formalin fixation, reporting a shrinkage factor of 0.8 when comparing post-MRI measurements with histopathologic invasion depth.

Regarding evaluation of regional nodal spread (N):

Detecting and differentiating between benign and malignant cervical lymph nodes is necessary for malignancy diagnosis, tumor staging, treatment planning, and follow-up. No imaging modality achieves sensitivity or specificity of 100%; therefore, neck dissection with histopathological examination remains the gold standard for nodal staging. (17)

In our study, N-staging was performed to assess lymph node metastasis. Conventional MRI, based on size, shape, extra capsular spread, and central necrosis, demonstrated an overall accuracy of 80.3%, whereas multi-parametric MRI improved the accuracy to 91.6%.

Liao et al. (18) performed a systematic review analyzing multiple trials that used conventional MRI for cervical lymph node metastasis detection in head and neck cancer cases between 2005 and 2010, reporting an average sensitivity of 65% and specificity of 81%.

Several studies suggest that ADC values obtained through DW-MRI can differentiate benign from metastatic nodes, even in small-sized nodes (19, 20).

However, some trials, such as those by Sumi et al. (21), found no statistically significant difference in ADC values among benign and metastatic nodes, especially in smaller nodes. Similarly, Heusch et al. (22) reported that incorporating DW-MRI didn't substantially enhance the diagnostic accuracy of PET-CT for detecting small metastatic nodes.

These findings highlight the potential of quantitative MRI in differentiating malignant from benign cervical nodes, potentially reducing the need for invasive procedures. However, further large-scale studies are required to validate these results in cervical lymph node metastases for primary oral or pharyngeal carcinomas.

Regarding detecting and differentiating of recurrent masses

In our study, the overall accuracy of conventional MRI for accurate identification of post treatment changes was 70.8%. While the use of multi parametric MRI modules, the overall accuracy improved be 85.5%.

In the study of Breik et al., (23) sensitivity of MRI in diagnosis of post treatment masses of oral and pharyngeal cancer was

60%. On the other hand, this disagreed with **Leel et al.,** (24) that were conducted on 21 cases were checked in the interval 3 months post irradiation and suspicious changes of tumor were present in 12 patients by conventional MRI. Only in 5 patients (42%) was tumor proved in histology.

DW-MRI has demonstrated value in differentiating recurrent head and neck malignancies from after-treatment changes. Jajodia et al. (25) reported a 94% sensitivity, 83.3% specificity, 93.6% accuracy, 95.9% PPV, and NPV of 83.3% for DW-MRI. Hwang et al. (26) found that DW-MRI differentiation between recurrent tumors and post-treatment changes in head and neck SCCs had 85% sensitivity, 84.6% specificity, and 84.8% accuracy. Becker et al. (27) studied local recurrence of SCC after radiotherapy and chemotherapy, finding that DW-MRI had a sensitivity of 93%, specificity of 93.5%, PPV of 90.9%, and NPV of 95.1%. Furukawa et al. (28) investigated the efficacy of dynamic contrast-enhanced MRI (DCE-MRI) at a 3-Tesla machine for head and neck masses, reporting that DCE-MRI achieved an 80% accuracy in differentiating malignant from benign tumors and a 100% accuracy in differentiating malignant tumors from post radiation changes.

Some studies have explored the combined use of MRI modalities to improve accuracy in distinguishing recurrent/residual tumors from post-therapeutic changes. Vaid et al. (29) illustrated that the overall diagnostic accuracy, PPV, and NPV of DW-MRI in distinguishing tumor recurrence from after-treatment changes were 84.3%, 86.8%, and 82.2%, respectively. When combining conventional MRI with quantitative ADC analysis, sensitivity, specificity, accuracy, PPV, and NPV improved to 90.13%, 82.5%, 86.4%, 84.4%, and 88.9%, respectively. Vandecaveye et al. (30) demonstrated that quantitative ADC analysis in DW-MRI, when combined with conventional MRI, yielded an overall accuracy of 95.5%, sensitivity of 94.6%, and specificity of 95.9%.

These findings reinforce the superior diagnostic capabilities of multi-parametric MRI in distinguishing benign from malignant lesions, staging malignant tumors, and assessing after treatment changes in cancers of head and neck.

5. CONCLUSION

The interpretation of multi parametric MRI use (conventional, diffusion and dynamic enhanced MRI) can advance the diagnostic accuracy of conventional MRI regarding nature of the masses, staging of malignant ones and discrimination of recurrent/ residual masses from post therapeutic changes. This improvement helps in the management strategy to reach maximal efficacy.

REFERENCES

[1] Varghese J, Kirsch C. Magnetic resonance imaging of the oral cavity and oropharynx. Topics in Magnetic Resonance Imaging. 2021;30(2):79-83.

[2] Cheng J, Shao S, Chen W, Zheng N. Application of Diffusion Kurtosis Imaging and Dynamic Contrast-Enhanced Magnetic Resonance Imaging in Differentiating Benign and Malignant Head and Neck Lesions. J Magn Reson Imaging. 2022;55(2):414-23.

[3] Razek AA, Elsebaie NA, Gamaleldin OA, AbdelKhalek A, Mukherji SK. Role of MR imaging in head and neck squamous cell carcinoma. Magn Reson Imaging Clin N Am. 2022;30(1):1-18.

[4] Kanmaz L, Karavas E. The role of diffusion-weighted magnetic resonance imaging in the differentiation of head and neck masses. J Clin Med. 2018;7(6):130.

[5] Singh A, Thukral CL, Gupta K, Sood AS, Singla H, Singh K. Role of MRI in evaluation of malignant lesions of tongue and oral cavity. Pol J Radiol. 2017;82:92.

[6] El Beltagi AH, Elsotouhy AH, Own AM, Abdelfattah W, Nair K, Vattoth S. Functional magnetic resonance imaging of head and neck cancer: Performance and potential. Neuroradiol J. 2019;32(1):36-52.

[7] Garbajs M, Strojan P, Surlan-Popovic K. Prognostic role of diffusion weighted and dynamic contrast-enhanced MRI in loco-regionally advanced head and neck cancer treated with concomitant chemoradiotherapy. Radiol Oncol. 2019;53(1): 39-48.

[8] Law CP, Chandra RV, Hoang JK, Phal PM. Imaging the oral cavity: key concepts for the radiologist. Br J Radiol. 2011;84(1006):944-57.

[9] Moreira MA, Lessa LS, Bortoli FR, Lopes A, Xavier EP, Ceretta RA, et al. Meta-analysis of magnetic resonance imaging accuracy for diagnosis of oral cancer. PLoS One. 2017;12(5):e0177462.

[10] Zhang SC, Zhou SH, Shang DS, Bao YY, Ruan LX, Wu TT. The diagnostic role of diffusion-weighted magnetic resonance imaging in hypopharyngeal carcinoma. Oncol Lett. 2018;15(4):5533-44.

[11] Dong Ji X, Yan S, Xia S, Guo Y, Shen W. Quantitative parameters correlated well with differentiation of squamous cell carcinoma at head and neck: a study of dynamic contrast-enhanced MRI. Acta Radiol. 2019;60(8):962-8.

[12] Park JO, Jung SL, Joo YH, Jung CK, Cho KJ, Kim MS. Diagnostic accuracy of magnetic resonance imaging

(MRI) in the assessment of tumor invasion depth in oral/oropharyngeal carcinoma. Am J Diagn Imaging. 2011;2(1):1-13.

[13] Alsaffar HA, Goldstein DP, King EV, De Almeida JR, Brown DH, Gilbert RW, et al. Correlation between clinical and MRI assessment of depth of invasion in oral tongue squamous cell carcinoma. J Otolaryngol Head Neck Surg. 2016;45(1):61.

[14] Guo N, Zeng W, Deng H, Hu H, Cheng Z, Yang Z, et al. Quantitative dynamic contrast-enhanced MR imaging can be used to predict the pathologic stages of oral tongue squamous cell carcinoma. BMC Med Imaging. 2020;20:1-9.

[15] Tang W, Wang Y, Yuan Y, Tao X. Assessment of tumor depth in oral tongue squamous cell carcinoma with multiparametric MRI: correlation with pathology. Eur Radiol. 2022;32:254-61.

[16] GOEL, Varun, et al. Accuracy of MRI in prediction of tumour thickness and nodal stage in oral tongue and gingivobuccal cancer with clinical correlation and staging. *Journal of clinical and diagnostic research: JCDR*, 2016, 10.6: TC01.

[17] Lee FKH, King AD, Ma BBY, Yeung DKW. Dynamic contrast enhancement magnetic resonance imaging (DCE-MRI) for differential diagnosis in head and neck cancers. Eur J Radiol. 2012;81(4):784-8.

[18] Liao LJ, Lo WC, Hsu WL, Wang CT, Lai MS. Detection of cervical lymph node metastasis in head and neck cancer patients with clinically N0 neck—a meta-analysis comparing different imaging modalities. BMC Cancer. 2012;12:1-7.

[19] Cintra MB, Ricz H, Mafee MF, Santos AC. Magnetic resonance imaging: dynamic contrast enhancement and diffusion-weighted imaging to identify malignant cervical lymph nodes. Radiol Bras. 2018;51(2):71-5.

[20] Zhou M, Lu B, Lv G, Tang Q, Zhu J, Li J, Shi K. Differential diagnosis between metastatic and non-metastatic lymph nodes using DW-MRI: a meta-analysis of diagnostic accuracy studies. J Cancer Res Clin Oncol. 2015;141(6):1119-30.

[21] Sumi M, Sakihama N, Sumi T, Morikawa M, Uetani M, Kabasawa H, et al. Discrimination of metastatic cervical lymph nodes with diffusion-weighted MR imaging in patients with head and neck cancer. Am J Neuroradiol. 2003;24(8):1627-34.

[22] Heusch P, Sproll C, Buchbender C, Rieser E, Terjung J, Antke C, et al. Diagnostic accuracy of ultrasound, 18 F-FDG-PET/CT, and fused 18 F-FDG-PET-MR images with DWI for the detection of cervical lymph node metastases of HNSCC. Clin Oral Investig. 2014;18(3):969-78.

[23] Breik O, Kumar A, Birchall J, Mortimore S, Laugharne D, Jones K. Follow up imaging of oral, oropharyngeal and hypopharyngeal cancer patients: comparison of PET-CT and MRI post treatment. J Craniomaxillofac Surg. 2020;48(7): 672-9.

[24] Lell M, Baum U, Greess H, Nömayr A, Nkenke E, Koester M, et al. Head and neck tumors: imaging recurrent tumor and post-therapeutic changes with CT and MRI. Eur J Radiol. 2000;33(3):239-47.

[25] Jajodia A, Aggarwal D, Chaturvedi AK, Rao A, Mahawar V, Gairola M, et al. Value of diffusion MR imaging in differentiation of recurrent head and neck malignancies from post treatment changes. Oral Oncol. 2019;96:89-96.

[26] Hwang I, Choi SH, Kim YJ, Kim KG, Lee AL, Yun TJ, et al. Differentiation of recurrent tumor and posttreatment changes in head and neck squamous cell carcinoma: application of high b-value diffusion-weighted imaging. Am J Neuroradiol. 2013;34(12):2343-8.

[27] Becker M, Varoquaux AD, Combescure C, Rager O, Pusztaszeri M, Burkhardt K, et al. Local recurrence of squamous cell carcinoma of the head and neck after radio (chemo) therapy: diagnostic performance of FDG-PET/MRI with diffusion-weighted sequences. Eur Radiol. 2018;28:651-63.

[28] Furukawa M, Anzai Y. Diagnosis of cervical lymph node metastasis in head and neck cancer: evidence-based neuroimaging. In: Evidence-Based Neuroimaging Diagnosis and Treatment: Improving the Quality of Neuroimaging in Patient Care. Cham: Springer; 2013. p. 693-718.

[29] Vaid S, Chandorkar A, Atre A, Shah D, Vaid N. Differentiating recurrent tumours from post-treatment changes in head and neck cancers: does diffusion-weighted MRI solve the eternal dilemma?. Clinical Radiology. 2017;72(1):74-83.

[30] Vandecaveye V, Dirix P, De Keyzer F, Op de Beeck K, Vander Poorten V, Roebben I, et al. Predictive value of diffusion-weighted magnetic resonance imaging during chemoradiotherapy for head and neck squamous cell carcinoma. Eur Radiol. 2010;20:1703-11.